

An investigation into the zooplankton composition of a prominent 38-kHz scattering layer in the North Sea

ANGUS M. MAIR¹*, PAUL G. FERNANDES¹, ANNE LÉBOURGÈS-DHAUSSY² AND ANDREW S. BRIERLEY³

¹FRS MARINE LABORATORY, PO BOX 101, 375 VICTORIA ROAD, ABERDEEN AB11 9DB, SCOTLAND, ²CENTRE IRD DE BRETAGNE, BP 70, 29280 PLOUZANÉ, FRANCE AND ³GATTY MARINE LABORATORY, UNIVERSITY OF ST. ANDREWS, ST. ANDREWS, FIFE KY16 8LB, SCOTLAND

*CORRESPONDING AUTHOR: a.mair@marlab.ac.uk

Received March 18, 2005; accepted in principle May 2, 2005; accepted for publication May 26, 2005; published online June 13, 2005

Communicating editor: K.J. Flynn

This study aims to determine the contribution made by zooplankton to acoustic scattering layers, which are particularly strong at 38 kHz, in the northern North Sea in summer. It uses a combination of net sampling and forward and inverse acoustic modelling of data collected at 38, 120 and 200 kHz in July 2003. Zooplankton samples were collected from regions of strong acoustic scattering in depths to ~50 m, using a undulating towed (U-tow) vehicle. Acoustic data recorded simultaneously were scrutinized to determine actual backscattering, expressed as mean volume backscattering strength (MVBS) (dB). This observed MVBS ($MVBS_{obs}$) was compared with backscattering predicted by application of appropriate acoustic models ($MVBS_{pred}$) to sampled densities of zooplankton. In all instances, $MVBS_{obs}$ was greater than $MVBS_{pred}$, with the difference considerably more pronounced at 38 kHz. There was a weak correlation between $MVBS_{pred}$ and $MVBS_{obs}$ at all three frequencies, with the greatest correlation ($r = 0.450$, $P = 0.545$) at 120 kHz. A number of candidate acoustic models were inverted in order to infer the most likely type of scatterer. In most cases, scatterers with a gas inclusion were predicted by this method. Potential sources of inconsistencies between $MVBS_{pred}$ and $MVBS_{obs}$ were identified which, when considered alongside the presented forward and inverse solutions, indicate that 38 kHz scattering in particular must be due to sources other than sampled zooplankton.

INTRODUCTION

The use of multifrequency acoustic technology in studies of zooplankton ecology is now commonplace. Acoustic sampling is essentially noninvasive and is operationally fast enough to distinguish patches at a number of scales both spatially and temporally (Holliday and Pieper, 1995). In most instances, however, it is still necessary to obtain physical samples to confirm the types of organism detected acoustically (MacLennan and Simmonds, 1992; Fielding *et al.*, 2004). Acoustic data can be used to direct nets to a patch of interest, improving the chances of directly sampling the acoustically detected targets (Greenlaw, 1979). Progressing from this, combined acoustic and net data can be used to generate acoustic-only species identification (Madureira *et al.*, 1993). Objective identification of certain animals via differences

in mean volume backscattering strength (MVBS) at different frequencies, without the need for biological sampling, has been postulated (Madureira *et al.*, 1993; Kang *et al.*, 2002; Korneliussen and Ona, 2002; Watkins and Brierley, 2002). Such procedures are based on the fact that different types of plankton (e.g. copepods, euphausiids and siphonophores) have diagnostic frequency responses (Holliday, 1977).

During acoustic surveys of herring in the North Sea (ICES area IVa) in summer, a strong 38 kHz scattering layer is present at a depth varying between ~10 and 75 m. This layer is less intense at 120 and 200 kHz (Fig. 1) and is often present for extended periods over the course of the survey. It has been generally but informally believed to consist of zooplankton. However, the layer composition has not been identified because it has not been sampled with plankton nets in the course of normal fish surveys.

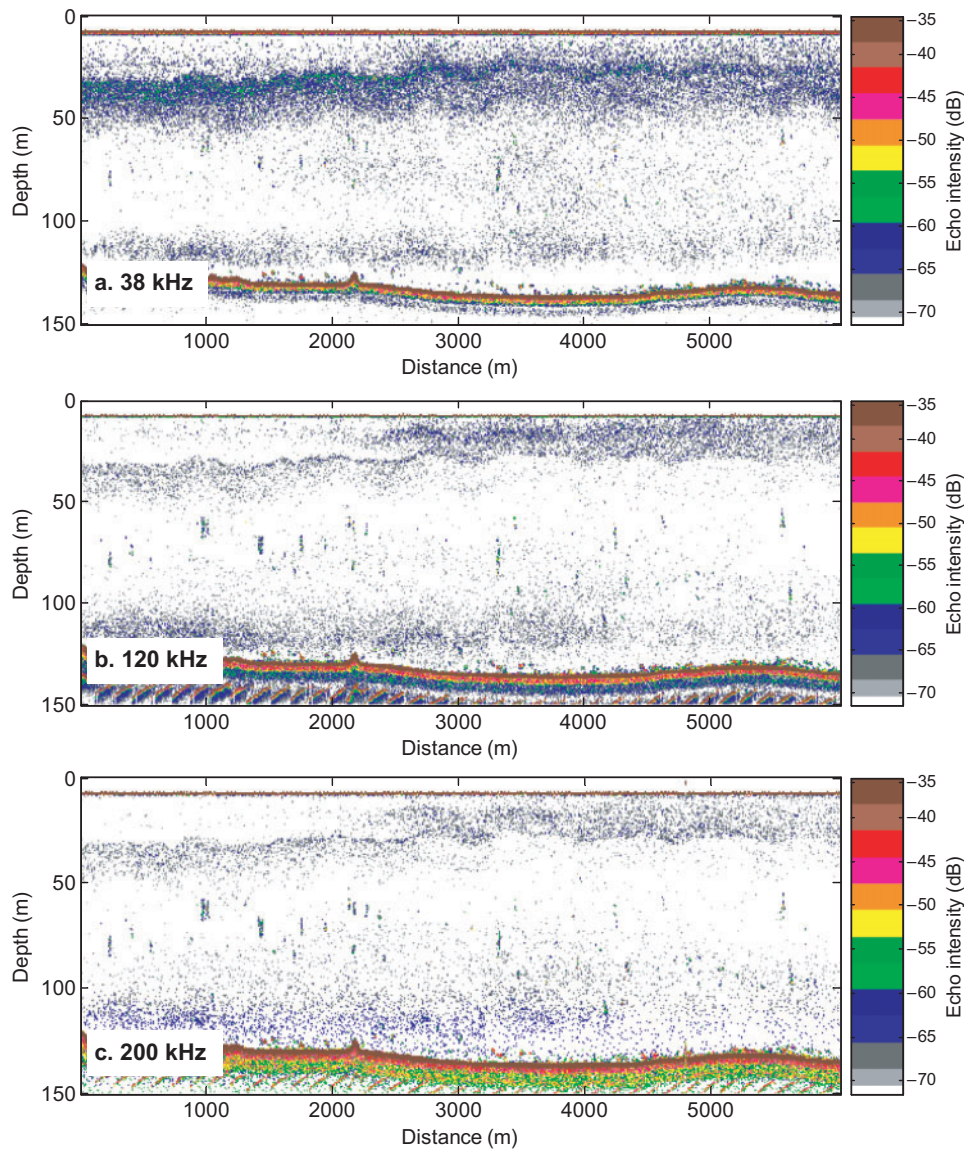


Fig. 1. Example echograms recorded at sound frequencies of (a) 38, (b) 120 and (c) 200 kHz on 1 July 2003 at $59^{\circ}33' \text{ N } 0^{\circ}50' \text{ W}$. Water depth is displayed on the left of each echogram and horizontal distance at the foot. Backscatter intensity is shown by use of colour, with the legend showing approximate decibel (dB) values for each colour used in the display. These echograms were recorded at a ship speed of ~ 10 knots. The scattering layer in question can be seen between the surface and ~ 60 m in this case.

The aim of this study was to identify the characteristics of acoustic scatterers contained in this layer using biological sampling and acoustic data recorded at 38, 120 and 200 kHz. Both forward (McNaught, 1968; Greenlaw, 1979) and inverse (Holliday, 1977; Greenlaw, 1979) methods were considered. A good overview of both has previously been published (Greenlaw and Johnson, 1983) but, in brief, the forward problem involves the sorting and identification of animals in the biological samples to determine their size and the basic shape by which they can be acoustically described (e.g. sphere). Acoustic scattering

models specific to those shapes (and other characteristics, such as size) are then applied to predict backscattering at each frequency. These predictions are then compared with simultaneously recorded acoustic data (Pieper and Holliday, 1984). The inverse method approaches the problem from the opposite direction, where the shape and size of the dominant scatterers are predicted from multifrequency backscattering. Originally (Holliday *et al.*, 1989; Pieper *et al.*, 1990), observed data were used to determine the most probable abundance for a given size of plankton of a single type. In this case, however, a range

of scattering models were inverted. This allows the type and size of the most likely scattering candidates among the expected types to be identified (LeBourges-Dhaussy and Ballé-Béganton, 2004).

Aside from the inherent scientific interest in the biological composition of a community of scatterers, proper identification of the targets causing the strong 38 kHz North Sea scattering layer will aid in the further development of algorithms, such as those suggested by Korneliussen and Ona (Korneliussen and Ona, 2002), that remove such targets from echograms. The ability to do this would have a beneficial effect on acoustic surveys of fish, where 38 kHz is the most commonly used sampling frequency (MacLennan and Simmonds, 1992), and when survey bias may arise either by evaluating plankton as fish or discarding fish echoes in the belief that they are caused by zooplankton.

METHOD

Zooplankton sample collection

An undulating towed (U-tow) vehicle equipped with a plankton sampling mechanism (PSM) similar to that found in the Longhurst-Hardy Plankton Recorder (LHPR) (Longhurst *et al.*, 1966) (Fig. 2) was deployed from the side deck of FRV ‘Scotia’ during the summer 2003 North Sea Herring Survey (ICES, 2004) to collect plankton samples. U-tow is a small, robust-bodied vehicle that can be deployed easily at ship speeds of up to twenty knots (Envirotech, 2003). A full description of the vehicle has been published by Cook and Hays (Cook and Hays, 2001).

A record was made of ship speed, time of deployment and recovery, depth of deployment and wire paid out for each haul. Hoses were attached to two of the five 18-mm circular apertures on the fore end of U-tow to direct water into the PSM. The PSM collected samples

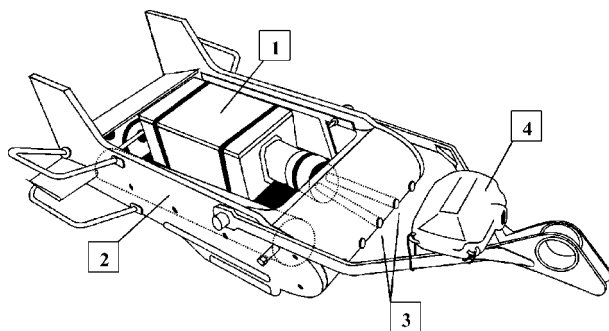


Fig. 2. Undulating Towed (U-tow) Vehicle. The vehicle is ~1 m long and contains a plankton sampling mechanism (PSM) unit (1) with a separate battery pack (2). Water is directed through the sampling apertures (3) and into the PSM. A SCANMAR depth unit (4) is attached in order to monitor and record sampling depth.

between two continuous 200- μ m meshes, which were wound onto a collection roller every 2 min. Operation of the PSM was observed on deck, and U-tow deployed immediately after the mesh was seen to wind on. Noting the time of this enabled the timing of subsequent samples to be calculated. Animals that entered the mechanism with the flow of water were trapped between the meshes, with individual samples identifiable on recovery by a ‘striping’ effect on the mesh. Samples were preserved in 4% formalin for identification later.

For most tows, the U-tow was deployed for multiples of 8 min at depths coinciding with a strong 38-kHz scattering layer observed on live-viewed echograms. By setting the trim on the U-tow and controlling the wire paid out, the vehicle was made to sample as close to horizontally as possible at the required depth rather than undulating across a range of depths. A calibrated depth sensor unit (SCANMAR HC4-D: Scanmar AS, Åsgårdstrand, Norway) attached to the U-tow operated during each deployment, enabling sampling depth to be determined to within 0.1 m at 1-min (300 m) intervals (Table I). Samples obtained

Table I: Description of U-tow hauls used in this study

U-tow haul identifier	Minimum depth (m)	Maximum depth (m)	Time of day start	Time of day end
003a	21.94	25.06	2141	2149
003b	19.56	20.31	2151	2159
004a	23.06	23.81	0615	0629
004b	39.69	41.25	0633	0647
005a	23.00	24.94	1155	1209
005b	48.19	49.06	1213	1219
005c	48.31	49.31	1220	1227
007a	19.12	25.75	1415	1429
007b	50.12	51.62	1433	1447
011a	19.88	21.62	0921	0935
0013	18.38	21.50	1716	1730
014a	25.88	27.12	1414	1428
014b	44.25	48.81	1432	1446
0016	23.06	23.88	1503	1517
017a	22.44	23.38	1740	1754
0022	45.62	47.44	1531	1545
023a	14.08	15.12	1833	1847
0024	21.06	26.62	0910	0924
0031	22.75	25.88	1859	1913
0036	29.50	30.88	0458	0512

All hauls came from ICES area IVa in July 2003. Start and end times indicate timing of actual sampling rather than deployment and recovery times. A SCANMAR depth unit reported the U-tow’s depth each minute. Maximum and minimum reported depths are shown.

from each tow were integrated so that each vial contained four samples collected over 8 min. The volume of water filtered was calculated by taking into account the size of U-tow's sampling apertures, the ship's speed (which was 10 knots for all hauls) and the sampling period.

Zooplankton sample analysis

Analysis of zooplankton samples was carried out in the laboratory after the cruise, using a binocular microscope. Calanoid copepods were analysed at least to genus, with *Calanus finmarchicus* to developmental stages C6 (adult) male/female and copepodite stages C4 and C5. Earlier developmental stages, along with *Acartia* spp., *Temora* spp. and other copepods <1.2 mm in length, were counted as 'small copepods <1.2 mm'. Other categories included Chaetognaths, Euphausiid juveniles, Decapod larvae, Cladocera, Cirripedia nauplii, Echinodermata larvae, Amphipoda and Polychaeta, although not all of these were found in all samples. Subsamples of up to 20 individuals from each category were measured to 0.01 mm for length and diameter using an eyepiece graticule, with mean values later used for modelling. Twenty hauls were analysed in this way.

For the purpose of this study, and taking into account the acoustic properties of different types and sizes of scatterers, *C. finmarchicus* C5 juveniles and other copepods >1.2 mm in length were considered together because of size similarities. *Calanus finmarchicus* adults (C6 stage) were considered separately, as were copepods <1.2 mm. Small euphausiids, polychaetes and chaetognaths were also considered separately, giving six categories of scatterer. The number of animals of each category per cubic metre of water was calculated from the number of animals caught and the volume of water filtered. Smaller animals (Cirripedia nauplii, Echinodermata larvae, early Decapoda larvae, Amphipoda and Cladocera) which were found to be few in number and not strong acoustic scatterers were disregarded at this stage.

Forward model predictions

Using the physical measurement and abundance data, the forward problem (Holliday and Pieper, 1995) was solved in order to predict backscattering values for each sample at each of the three frequencies using Distorted Wave Born Approximation (DWBA) models (Stanton and Chu, 2000). Density contrast (g), sound speed contrast (h) and animal orientation parameter values were set as outlined in Table II, using published values (Stanton and Chu, 2000) with further advice from G. Lawson and D. Chu (G. Lawson and D. Chu, Wood's Hole Oceanographic Institute, USA, personal communication).

Table II: Model parameters used in forward calculations

	g	h	Orientation (°)
Copepod	1.02	1.058	0 ± 30
Euphausiid	1.016	1.019	20 ± 20
Polychaete	1.03	1.03	0 ± 30
Chaetognath	1.03	1.03	0 ± 30

Density contrast ratio (g), sound speed contrast ratio (h) and the mean and SD of angles of animal orientation (in degrees) are given for the four scatterer types under consideration.

The three categories of copepods were treated as fluid-filled prolate spheroids. Euphausiids, chaetognaths and polychaetes were treated as fluid-filled, bent cylinders.

In order to allow direct comparison with recorded acoustic data, model-output target strength (TS) values were converted to *MVBS* using the following equation:

$$MVBS_{\text{pred}} = TS + 10 \log_{10}(n) \quad (1)$$

where $MVBS_{\text{pred}}$ is the predicted mean volume backscattering strength (dB), TS is the target strength output of the relevant model (dB) and n is the calculated number of animals per cubic metre of seawater for the relevant species group.

This calculation was performed for all six scattering categories, and the resultant values added in the linear domain to give a total $MVBS_{\text{pred}}$ for each haul. The dominant group of sampled scatterers for each haul at each frequency was identified as that which made the greatest contribution to total $MVBS_{\text{pred}}$ (either 'spheroid' or 'cylinder'—scatterer types not found in samples could not be included in this calculation).

Acoustic data collection and analysis

Acoustic data were obtained simultaneously with net samples using a SIMRAD EK500 scientific echo sounder transmitting and receiving via transducers positioned at a depth of 8.6 m on Scotia's drop keel at 38 (single beam, 7° beam width), 120 (split-beam, 7° beam width) and 200 (single beam, 7° beam width) kHz. Prior to sampling, the echo sounder was calibrated using standard sphere techniques (Foote *et al.*, 1987). Pings were transmitted every 1.5 s with a pulse duration of 1 ms for each frequency. Acoustic signals were digitized and processed by the EK500 (20 log R TVG and calibration gains applied) and volume backscattering strength data (S_v in dB re. 1 m^{-1}) were logged for post-processing. Using SonarData Echoview software (SonarData Pty, GPO Box 1387, Hobart, Tasmania, Australia), acoustic

data were scrutinized in the form of calibrated echograms. Each pixel on these echograms represented an area of 7.5 m horizontally and 3.5 m vertically. Regions of echograms corresponding to U-tow's position in the water at the time of each haul were identified using SCANMAR depth data, haul start/end times and amount of warp paid out. For example, when U-tow operated at 25-m depth it was typically 150 m behind the vessel, so a delay of 30 s was needed to align acoustic data with U-tow's position.

An 'observed' mean volume backscatter strength ($MVBS_{\text{obs}}$) value for each defined haul region was obtained via echo integration at each of the three frequencies.

$MVBS_{\text{pred}}$ was compared with $MVBS_{\text{obs}}$ and correlation coefficients calculated for each frequency. In order to find whether low correlations were caused by simple undersampling of the zooplankton community, $MVBS_{\text{pred}}$ values were calculated for multiples of sampled animal abundances and compared with $MVBS_{\text{obs}}$.

Inverse model predictions

The inverse problem was solved for 10 of the hauls with the aim of identifying the expected dominant scatterer in each region according to scattering characteristics at the frequencies used. Inverse processing of acoustic data outputs the single type of scatterer which dominates acoustic reflection in each data bin. Bearing this in mind, we divided the area of each haul into smaller sampling volumes for this procedure in order to get an indication of the diversity of organisms present. Haul regions on echograms were divided into cells corresponding to areas of the water column 150 m in length (equating to 15 acoustic pings) and 2 m in depth. Owing to the nature of the inverse method, which fits theoretical models to data, scatterer types other than those sampled—such as gas-bearing plankton—were considered as potential candidates. For each cell, the inversion process fits models to the $MVBS$ values measured at 38, 120 and 200 kHz. The available models include Truncated Fluid-Filled Sphere (Costello *et al.*, 1989), DWBA Fluid-Filled Prolate Spheroid (D. Chu and G. Lawson, Wood's Hole Oceanographic Institute, USA, personal communication), DWBA Fluid-Filled Bent Cylinder (Stanton and Chu, 2000), High-Pass Elastic Shelled (Stanton *et al.*, 1994) and High-Pass Gaseous Sphere (Stanton, 1989). Solution of the inverse problem provides a possible population composition which, were the forward problem to be solved for it, would have a calculated $MVBS$ as close as possible to measured $MVBS$ in a least squares sense. The following error norm is calculated:

$$\text{Error} = \sqrt{\sum_{i=1}^n [S_v^{\text{calculated}}(f_i) - S_v^{\text{measured}}(f_i)]^2} \quad (1)$$

where n is the total number of measured frequencies, and S_v (volume backscattering coefficient) is as $MVBS = 10 \log(S_v)$.

The model that provides the lowest error is considered as that which most closely matches the observed values. This was taken to be an indicator of dominant scatterer type in each cell.

RESULTS

Six categories of scatterers (*Calanus finmarchicus* C6 and C5, copepods <1.2 mm, chaetognaths, polychaetes and euphausiids) accounted for over 95% of animals by number in all samples, and over 99% in most. Other animals found in small numbers included Cladocera, Cirripedia nauplii and fragments of gelatinous animals. Fish larvae and elastic-shelled molluscs were noticeably absent in the samples.

Measurements were made of a subsample of animals ($n = 20$) from each category found in each sample. Table III gives mean length with standard deviation, length to cylindrical radius ratio (L/a), and average $MVBS_{\text{pred}}$ at each frequency (38, 120 and 200 kHz) data combined from all hauls. Abundance values for each category varied considerably from haul to haul.

As may be expected due to their greater size, adult *C. finmarchicus* were the dominant sampled scatterer among spheroid-type animals in all hauls and contributed the highest percentage of total backscatter in twelve of the twenty hauls. In the same way, Euphausiids were generally found to be the scatterer among cylinder types that dominated backscatter, despite the often far greater abundance of Chaetognaths and Polychaetes. Cylinder-type animals were the overall dominant sampled scatterers in four hauls at all three frequencies. In the remaining four hauls, neither type dominated. It should be noted that candidates for the dominant 'sampled' scatterer included only those animal types which were found in samples and not other possibilities such as gas-bearing particles, which were not present in net samples.

Overall $MVBS_{\text{pred}}$ was compared with recorded $MVBS_{\text{obs}}$ for each haul (Fig. 3a, b and c), and correlation coefficients obtained (38 kHz $r = 0.144$, $P = 0.545$; 120 kHz $r = 0.450$, $P = 0.046$; 200 kHz $r = 0.365$, $P = 0.114$). $MVBS_{\text{pred}}$ was lower than $MVBS_{\text{obs}}$ for all hauls and at all three frequencies, with the difference most pronounced at 38 kHz.

Table III: Average predicted mean volume backscattering strength (MVBS) at 38, 120 and 200 kHz for the six scatterer types identified in samples

Species group	Averages across all hauls					
	Mean length (mm)	SD	L/a	38 kHz $MVBS_{pred}$ (dB)	120 kHz $MVBS_{pred}$ (dB)	200 kHz $MVBS_{pred}$ (Db)
Spheroid type						
<i>Calanus finmarchicus</i> C6	2.30	0.06	3.2	-108.94	-89.79	-82.60
<i>C. finmarchicus</i> C5	1.98	0.10	3.2	-116.52	-97.15	-89.51
Copepods <1.2 mm	0.39	0.09	3.2	-146.13	-126.18	-117.35
Cylinder type						
Euphausiids	5.58	2.64	6.7	-93.17	-78.14	-73.46
Polychaetes	1.31	1.04	8.0	-124.47	-107.68	-100.49
Chaetognaths	7.55	2.54	18.0	-118.34	-101.46	-93.59

The animal length and MVBS data shown are average values (with SD) calculated across all hauls for each of the six categories. Mean length and length to cylindrical radius ratios (L/a) were calculated from measurements of sampled animals.

The most noticeable difference between $MVBS_{obs}$ and $MVBS_{pred}$ is the relationship between 38 and 120 kHz (Fig. 4). Curves were fitted to each set of three points in Fig. 4 in order to aid visual interpretation of relative scattering levels. The curve for observed values has a decreasing trend between 38 and 120 kHz, whilst that for predicted values increases. Artificially doubling the abundance of sampled animals and then applying scattering models gave $MVBS_{pred}$ values which closely approached $MVBS_{obs}$ at 120 and 200 kHz. However, a 200-fold increase in abundance was required to give $MVBS_{pred}$ values close to $MVBS_{obs}$ at 38 kHz. Such an increase gave $MVBS_{pred}$ values at 120 and 200 kHz which were far greater (~20 dB) than $MVBS_{obs}$ at those frequencies (Fig. 4).

Solution of the inverse problem identified a single theoretical dominant scatterer type for each echogram cell in 10 of the hauls. Table IV shows the scatterer types which dominated backscatter according to solution of both forward and inverse problems for these hauls. The inverse method predicts the presence of scatterers with a gas inclusion in all except two hauls, where elastic-shelled scatterers are predicted. Neither type of scatterer featured in biological samples collected by the U-tow.

Although the scatterer type having the greatest influence on total backscatter can be identified separately for each frequency by solving the forward problem, the model-fitting nature of the inverse method requires data from all three frequencies and therefore outputs only a single solution for each echogram cell. In most cells, the acoustic data most closely fit the model for ‘gaseous sphere’ (~0.1–0.4 mm) type scatterers. Two hauls (003a and 014a) were dominated by ‘fluid prolate

spheroid’ (~1.4 mm) with some amount of ‘gaseous sphere’ (~0.1 mm), and one (0014b) showed ‘fluid prolate spheroid’ as dominant with some ‘elastic shelled’ (~1.4 mm) type.

Using physical animal measurements, and treating all animals as cylinders, biovolume for each haul was calculated. Table IV shows which type of animal contributed most to each haul as a percentage of total sample biovolume calculated in this way.

DISCUSSION

Zooplankton sampling regime

There was a large mismatch between predicted and observed backscatter at 38 kHz for most of our hauls, which we attribute to selective net sampling. The PSM collects samples on a continuous mesh system. In this study, it was installed in a U-tow vehicle with circular sampling apertures of 18 mm diameter and towed at a normal survey speed of 10 knots. The size of the sampling apertures immediately precludes the capture of larger animals. It may be expected that some fish larvae, also potentially strong 38 kHz scatterers, were present in the area of sampling. Cod larvae, for example, are found in the North Sea from March to September (Beaugrad *et al.*, 2003), and the spawning times of other species such as haddock and whiting (Coull *et al.*, 1998) suggest that larvae may be present. The total lack of these in any of the samples suggests that they either avoided the vehicle or were deflected away from the sampling apertures by its bow wave. Siphonophores, another potentially strong scatterer at the frequencies under consideration (Benfield *et al.*, 2003), were also absent from the samples, although

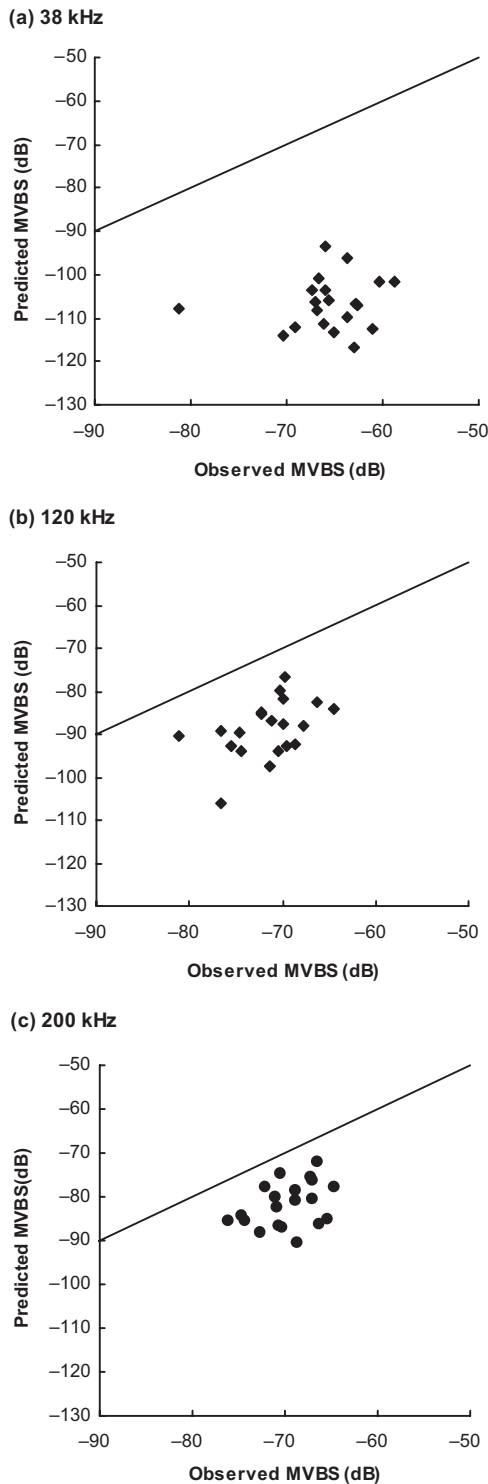


Fig. 3. Predicted mean volume backscattering strength ($MVBS$) plotted against observed $MVBS$ at (a) 38 kHz, (b) 120 kHz and (c) 200 kHz. A line corresponding to a 1:1 relationship is shown on each plot. For all hauls at all frequencies, predicted $MVBS$ was less than observed $MVBS$.

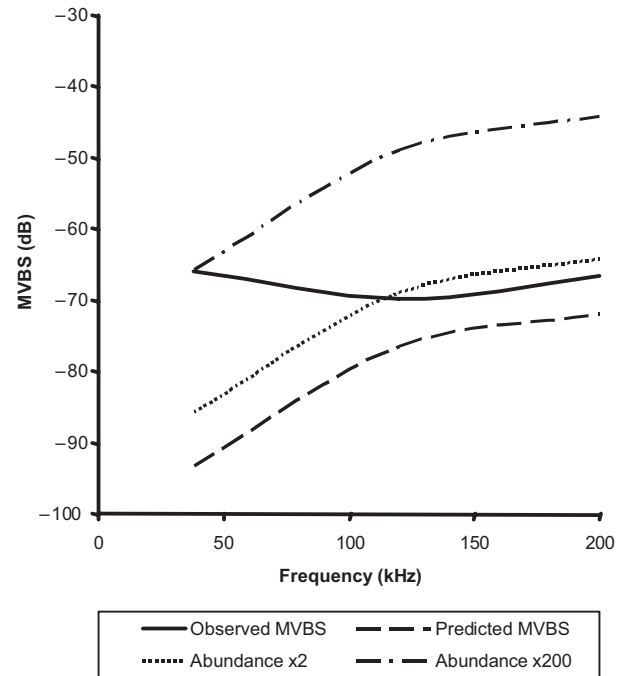


Fig. 4. Predicted mean volume backscattering strength ($MVBS_{pred}$) for one haul according to sampled zooplankton (dashed line), and the predicted increase in $MVBS$ caused by $\times 2$ (dotted line) and $\times 200$ (dash-dot line) sampled animal abundance. The solid line shows observed $MVBS$.

pieces of gelatinous material were occasionally found. It is possible that such animals were destroyed by the mechanism of the sampler and thus rendered unidentifiable. Larger gelatinous animals, such as *Aurelia aurita* and *Cyanea* spp., which may have been present and have similar anatomies to gelatinous species that have been shown to be strong acoustic targets at 38 kHz (Brierley *et al.*, 2001), were simply too large to be sampled.

Previous trials by the authors which compared the performance of U-tow with the ARIES plankton sampler (Dunn *et al.*, 1993) appeared to confirm that U-tow sampled the zooplankton community effectively in that the same types of animals were found in samples from both, although the number of animals sampled by ARIES was often an order of magnitude higher (unpublished results, Mair, 2003). Similar results were found by Cook and Hays (Cook and Hays, 2001) when comparing U-tow's sampling capabilities with a WP2 net.

By artificially increasing zooplankton abundance values, the product of the forward problem, $MVBS_{pred}$, can be forced to approach $MVBS_{obs}$ more closely, with an increase of 5–10 dB in $MVBS_{pred}$ resulting in a closer correlation with $MVBS_{obs}$ at 120 and 200 kHz. Such an increase is possible with a doubling of our sampled animal abundance at the same species composition, but

Table IV: Dominant scatterer types as identified by forward and inverse problems

Haul number	Sampled zooplankton biovolume ($\text{mm}^3 \text{m}^{-3}$)	Animal type dominant in catch (% of biovolume) (scatterer type)	Frequency (kHz)	Forward problem (dominant scatterer at each frequency)	Inverse problem [dominant scatterers with approximate ESR (mm)]
003a	62.0	Euphausiids (68%)	38	Cylinder	Fluid prolate spheroid (1.4 mm), gaseous sphere (0.1 mm)
003a			120	Cylinder	
003a			200	Cylinder	
004b	6.7	Copepods >1.2 mm (73%)	38	Cylinder	Gaseous sphere (0.1 mm), some fluid prolate spheroid (1.4 mm)
004b			120	Cylinder	
004b			200	Spheroid	
005a	4.2	Copepods >1.2 mm (58%)	38	Spheroid	Gaseous sphere (0.1 mm), some fluid prolate spheroid (1.4 mm)
005a			120	Spheroid	
005a			200	Spheroid	
007a	19.8	Copepods >1.2 mm (57%)	38	Spheroid	Gaseous sphere (0.1 mm)
007a			120	Spheroid	
007a			200	Spheroid	
007b	29.4	Euphausiids (46%)	38	Cylinder	Gaseous sphere (0.1 mm), some fluid prolate spheroid (1.4 mm)
007b			120	Cylinder	
007b			200	Cylinder	
011a	6.4	Copepods >1.2 mm (50%)	38	Spheroid	Gaseous sphere (0.1 mm)
011a			120	Spheroid	
011a			200	Spheroid	
0013	3.5	Copepods >1.2 mm (54%)	38	Spheroid	Fluid prolate spheroid (1.4 mm), elastic shelled (1.4 mm)
0013			120	Spheroid	
0013			200	Spheroid	
0014a	33.3	Copepods >1.2 mm (64%)	38	Cylinder	Fluid prolate spheroid (1.4 mm), gaseous sphere (0.1 mm)
0014a			120	Spheroid	
0014a			200	Spheroid	
0014b	4.6	Euphausiids (47%)	38	Cylinder	Fluid prolate spheroid (1.4 mm), elastic shelled (1.4 mm)
0014b			120	Cylinder	
0014b			200	Cylinder	
0036	7.0	Copepods >1.2 mm (44%)	38	Spheroid	Gaseous sphere (0.1 mm)
0036			120	Spheroid	
0036			200	Spheroid	

For the forward problem, dominant scatterer type is given for each frequency. All three frequencies are used in arriving at solutions for the inverse problem, for which the best fit was found at the equivalent spherical radius (ESR) shown in each case. The total biovolume of sampled animals in each haul and the type of animal which contributed most to this is also shown

this artificial method of moving predicted closer to observed values does not solve the difference in 'curve' trend between 38 and 120 kHz. Similar manipulation of abundance results in an $MVBS_{pred}$ value at 38 kHz which is still around 20 dB lower than $MVBS_{obs}$ at that frequency. It can be said with some confidence, therefore, that simple under-sampling of the zooplankton community is not responsible for the difference between $MVBS_{pred}$ and $MVBS_{obs}$ at 38 kHz—rather, we must be failing to catch scatterers that give strong echoes at 38 kHz. These are likely to be non-crustacean zooplankton, fish or physical objects such as bubbles.

The most likely candidate scatterers that we failed to sample by net are those containing some form of gas inclusion, including small or larval fish with a developed swim bladder, siphonophores, other gas-bearing animals or some combination of these. There is a lack of published data relating larval or postlarval fish to strong 38-kHz scattering layers, but the presence of such a layer coinciding with samples containing small fish has been observed (M. Heath, FRS Marine Laboratory, Aberdeen, Scotland, personal communication). Larger, swim-bladder-less fish may also have been present.

It has been suggested that the presence of gas vacuoles in phytoplankton cells increases their TB considerably at frequencies of 10–30 kHz (Selivanovsky *et al.*, 1996). Traces of phytoplankton were found in our samples, but the abundance could not be measured quantitatively.

Hydrodynamic wakes of animals such as squid and fish are reported to contain gas bubbles formed either by cavitation due to pressure drop or, in the case of the former, by the inclusion of phytoplankton cells containing gas in expelled jets of water (Selivanovsky and Ezersky, 1996). However, the characteristic linear traces produced by such wakes were not detected on the echograms here.

Additionally, many kinds of plankton from bacteria to large jellyfish produce exudates and excreta as byproducts of feeding and metabolism. Most often these consist of sticky mucosubstances which then aggregate to form marine snow. Such aggregations can be very numerous in the sea and are quickly colonized by bacteria and microflagellates. These break down the substances and particles trapped within the matrix and add their own exudates and metabolic byproducts (Kjørboe, 2001). Marine snow does not always simply sink as any gas trapped in the matrix can result in varying degrees of buoyancy. Indeed, the aggregations may also trap bubbles rising from sediments or mixed down from surface waves. Such flocs are usually so fragile that nets are incapable of effectively sampling them. However, they must be considered as a potential source of scattering.

Elastic-shelled molluscs, identified by the inverse problem as an important scatterer type in one haul and present scatterers in two other hauls, may have been present in the water column but were not sampled. Such animals, e.g. *Limacina* spp., appear commonly in North Sea zooplankton samples (J. Dunn, FRS Marine Laboratory, Aberdeen, Scotland, personal communication) and have a greater TS than the types of animals which were sampled (Stanton *et al.*, 1996).

It may even be that potential scatterers (e.g. gaseous types) have no biological origin but are rather the result of some physical hydrographical process. This seems unlikely as shipboard observation shows that the layer appears to migrate diurnally.

In this study, the sampling limitations of the U-tow vehicle have become apparent. Of primary concern are the small sampling apertures and the mechanics of sample collection within the PSM—resulting respectively in avoidance of the vehicle or destruction of animals on the mesh. Results show that the collected samples are not representative of the total scattering population, either due to under-sampling or an inability to sample a part of that population. The results of the forward and inverse problems show that possible under-sampling is more likely to affect our results at 120 and 200 kHz, whilst strong 38 kHz scatterers do not seem to have been sampled at all.

Forward model predictions

$MVBS_{pred}$ values were lower than $MVBS_{obs}$ in all cases. This is to be expected because net samples are unlikely to contain all scatterers sampled acoustically. $MVBS_{pred}$ was significantly correlated with $MVBS_{obs}$ at 120 kHz, whilst at 38 and 200 kHz only a weak correlation was found (38 kHz $r = 0.144$, $P = 0.545$; 120 kHz $r = 0.450$, $P = 0.046$; 200 kHz $r = 0.365$, $P = 0.114$). This suggests that the numbers of organisms sampled are proportionally representative of those that are strong scatterers at 120 kHz. For example, 120-kHz scattering layers are strongly associated with mesozooplankton (smaller than krill) in the Southern Ocean (Brierley and Watkins, 1996).

It should also be noted that assumptions were made when comparing $MVBS_{pred}$ and $MVBS_{obs}$ values. It was assumed that the same population was sampled biologically and acoustically. Acoustic data recorded in the region of each haul were defined as accurately as possible according to sampler depth and distance behind the ship. At a speed of 10 knots, however, the deployed sampler travelled through the water column at a distance of up to 450 m (~1.5 minutes) behind the ship's transducers. Thus, acoustic and biological data are unlikely to have been matched exactly. It should also be

noted that it is possible that rarely occurring strong scatterers represented in the acoustic data will not be biologically sampled. Fielding *et al.* (Fielding *et al.*, 2004), for example, reported that a single pteropod represented 69.5% of model-predicted backscattering yet only 0.1% of sampled biovolume.

Parameters used in the predictive acoustic modelling may require further investigation. In addition to problems with species composition, errors may arise due to the values for density contrast (*g*), sound speed contrast (*h*) and animal orientation used in models. Values we have used may not be wholly appropriate for the types of zooplankton under consideration in the North Sea. There are limited published data on the subject of density and sound-speed contrast in zooplankton, none of which involve animals sourced from the North Sea (Chu and Copley, 2000; Chu and Wiebe, 2005), and an acknowledged difficulty in determining *in situ* animal orientation (Foote and Stanton, 2000).

Inverse model predictions

Solution of the inverse problem for 10 of the hauls showed in most cases that acoustic data most closely corresponded to expectations for gaseous spheres, with two hauls containing cells most closely matching the fluid prolate spheroid model mixed with cells matching the gaseous sphere model, and one haul most closely matching the fluid prolate spheroid model mixed with the elastic-shelled model. This would appear to confirm the suggestions above that the dominant scatterer, that was not sampled biologically, generally contained some form of gas inclusion.

CONCLUSION

The evidence presented here indicates that mesozooplankton alone cannot be responsible for the strong 38-kHz scattering layer in the North Sea in summer. Artificial manipulation of sampled animal abundances showed that many more animals of the types sampled were required to account for scattering at 38 kHz than at 120 or 200 kHz. Application of the inverse method suggested that some form of gaseous sphere type scatterer was present, but such scatterers were not found in samples. With this in mind, biological and acoustic sampling were repeated in the summer of 2004 using a Methot Isaac-Kidd Trawl (MIKT) net in place of the U-tow/LHPR-type PSM. This apparatus should be more successful than the U-tow in catching certain types of sound-scatterers. Initial observation of samples obtained showed that fish larvae were present, as

were elastic-shelled molluscs and large scyphozoan medusae, each of which are possible candidates that may contribute to this phenomenon.

ACKNOWLEDGEMENTS

We are grateful to Gareth Lawson and Dezhong Chu of Woods Hole Oceanographic Institute (WHOI), Woods Hole, MA, USA for assistance with the latest versions of acoustic backscatter models and John Dunn of FRS Marine Laboratory, Aberdeen for his ongoing help with plankton sampling devices. Steve Hay and Mike Heath, also of FRS Marine Laboratory, provided us with information which was a great help. Finally, we acknowledge the reviewers whose comments improved the manuscript.

This document was made with support from the European Commission's Fifth Framework Programme (SIMFAMI project; Grant No. Q5RS-2001-02054).

REFERENCES

- Beaugrad, G., Brander, K. M., Lindley, J. A. *et al.* (2003) Plankton effect on cod recruitment in the North Sea. *Nature*, **426**, 661–664.
- Benfield, M. C., Lavery, A. C., Wiebe, P. H. *et al.* (2003) Distributions of physonect siphonulae in the Gulf of Maine and their potential as important sources of acoustic scattering. *Can. J. Fish. Aquat. Sci.*, **60**, 759–772.
- Brierley, A. S., Axelsen, B. E., Buecher, E. *et al.* (2001) Acoustic observations of jellyfish in the Namibian Benguela. *Mar. Ecol. Prog. Ser.*, **210**, 55–66.
- Brierley, A. S. and Watkins, J. L. (1996) Acoustic targets at South Georgia and the South Orkney Islands during a season of krill scarcity. *Mar. Ecol. Prog. Ser.*, **138**, 51–61.
- Chu, D. and Copley, N. (2000) Inference of material properties of zooplankton from acoustic and resistivity measurements. *ICES J. Mar. Sci.*, **57**, 1128–1142.
- Chu, D. and Wiebe, P. H. (2005) Measurements of acoustic material properties of zooplankton in Antarctic waters. *ICES J. Mar. Sci.*, **62**, 818–831.
- Cook, K. B. and Hays, G. C. (2001) Comparison of the epipelagic zooplankton samples from a U-Tow and the traditional WP2 net. *J. Plankton Res.*, **23**, 953–962.
- Costello, J. H., Pieper, R. E. and Holliday, D. V. (1989) Comparison of acoustic and pump sampling techniques for the analysis of zooplankton distributions. *J. Plankton Res.*, **11**, 703–709.
- Coull, K. A., Johnstone, R. and Rogers, S. I. (1998) *Fisheries Sensitivity Maps in British Waters*. UKOOA, Aberdeen, Scotland.
- Dunn, J., Hall, C. D., Heath, M. R., *et al.* (1993) ARIES – a system for concurrent physical, biological and chemical sampling at sea. *Deep-Sea Res.* **40**, 867–878.
- Envirotech (2003) U-Tow: Undulating Towed Vehicle. Corporate information leaflet.
- Fielding, S., Griffiths, G. and Roe, H. S. J. (2004) The biological validation of ADCP acoustic backscatter through direct comparison

- with net samples and model predictions based on acoustic-scattering models. *ICES J. Mar. Sci.*, **61**, 184–200.
- Corporate information leaflet J. (1987) Calibration of acoustic instruments for fish density estimation: a practical guide. *ICES Cooperative Research Report*, **144**.
- Foote, K. G. and Stanton, T. K. (2000) Acoustical methods. In Harris, R., Wiebe, P., Lenz, J., Skjoldal, H. and Huntley M. (eds), *ICES Zooplankton Methodology Manual*. Academic, London, pp. 223–258.
- Greenlaw, C. F. (1979) Acoustical estimation of zooplankton populations. *Limnol. Oceanogr.*, **24**, 226–242.
- Greenlaw, C. F. and Johnson, R. K. (1983) Multiple frequency acoustical estimation. *Biol. Oceanogr.*, **2**, 227–252.
- Holliday, D. V. (1977) Extracting bio-physical information from acoustic signatures of marine organisms. In Anderson, N. R. and Zahuranec, B. J. (eds), *Oceanic Sound Scattering Prediction*. Plenum Press, New York, pp. 619–624.
- Holliday, D. V. and Pieper, R. E. (1995) Bioacoustical oceanography at high frequencies. *ICES J. Mar. Sci.*, **52**, 279–296.
- Holliday, D. V., Pieper, R. E. and Kleppel, G. S. (1989) Determination of zooplankton size and distribution with multi-frequency acoustic technology. *J. Cons. Int. Explor. Mer.*, **46**, 52–61.
- ICES (2004) *Report of the Planning Group for Herring Surveys*, **ICES CM 2004/G:05**, pp. 7–9.
- Kang, M., Furusawa, M. and Miyashita, K. (2002) Effective and accurate use of difference in mean volume backscattering strength to identify fish and plankton. *ICES J. Mar. Sci.*, **59**, 794–804.
- Kjørboe, T. (2001) Formation and fate of marine snow: small-scale processes with large-scale implications. *Sci. Mar.*, **65** (Suppl. 2), 57–71.
- Korneliussen, R. J. and Ona, E. (2002) An operational system for processing and visualizing multi-frequency acoustic data. *ICES J. Mar. Sci.*, **59**, 293–313.
- LeBourges-Dhaussy, A. and Ballé-Béganton, J. (2004) *Multifrequency Multimodel Zooplankton Classification*. **ICES CM 2004/R: 22**.
- Longhurst, A. R., Reith, A. D., Bower, R. E. *et al.* (1966) A new system for the collection of multiple serial plankton samples. *Deep-Sea Res.*, **13**, 213–222.
- MacLennan, D. N. and Simmonds, E. J. (1992) *Fisheries Acoustics*. Chapman & Hall, London, 325 pp.
- Madureira, L. S. P., Everson, I. and Murphy, E. J. (1993) Interpretation of acoustic data at two frequencies to discriminate between Antarctic krill (*Euphausia superba* Dana) and other scatterers. *J. Plankton Res.*, **15**, 787–802.
- McNaught, D. C. (1968) Acoustical determination of zooplankton distributions. *Proceedings of the 12th Conference on Great Lakes Research*. 61–68.
- Pieper, R. E. and Holliday, D. V. (1984) Acoustic measurements of zooplankton distributions in the sea. *J. Cons. Int. Explor. Mer.*, **41**, 226–238.
- Pieper, R. E., Holliday, D. V. and Kleppel, G. S. (1990) Quantitative zooplankton distributions from multifrequency acoustics. *J. Plankton Res.*, **12**, 433–441.
- Selivanovsky, D. A. and Ezersky, A. B. (1996) Sound scattering by hydrodynamic wakes of sea animals. *ICES J. Mar. Sci.*, **53**, 377–381.
- Selivanovsky, D. A., Stunzhas, P. A. and Didenkulov, I. N. (1996) Acoustical investigation of phytoplankton. *ICES J. Mar. Sci.*, **53**, 313–316.
- Stanton, T. K. (1989) Simple approximate formulas for backscattering of sound by spherical and elongated objects. *J. Acoust. Soc. Am.*, **86**, 1499–1510.
- Stanton, T. K. and Chu, D. (2000) Review and recommendations for the modelling of acoustic scattering by fluid-like elongated zooplankton: euphausiids and copepods. *ICES J. Mar. Sci.*, **57**, 793–807.
- Stanton, T. K., Chu, D. and Wiebe, P. H. (1996) Acoustic scattering characteristics of several zooplankton groups. *ICES J. Mar. Sci.*, **53**, 289–295.
- Stanton, T. K., Wiebe, P. H., Chu, D. *et al.* (1994) On acoustic estimates of zooplankton biomass. *ICES J. Mar. Sci.*, **51**, 505–512.
- Watkins, J. L. and Brierley, A. S. (2002) Verification of the acoustic techniques used to identify Antarctic krill. *ICES J. Mar. Sci.*, **59**, 1326–1336.

